Tikrit Journal of Engineering Sciences (2025); 32(2): 1876

DOI: http://doi.org/10.25130/tjes.32.2.16

IRAQI Academic Scientific Journals

ISSN: 1813-162X (Print); 2312-7589 (Online)

Tikrit Journal of Engineering Sciences

available online at: http://www.tj-es.com

TJES Tikrit Journal of Engineering Sciences

Crystal Violet Dye Removal from Aqueous Solution Using Corn Silks as an Environmentally Friendly Adsorbent

Israa Sabeeh Al-Bayati [a], *Basma I. Waisi* *[a], *Manal A. Mohammed* [a], *Asrar A. Alobaidy* [a], *Mohammed A. Kadhom* [b]

a Department of Chemical Engineering, College of Engineering, University of Baghdad, Baghdad, Iraq.

b Department of Environmental Science, College of Energy and Environmental Sciences, Alkarkh University of Science, Baghdad, 10081, Iraq.

Keywords:

Adsorption; Corn silks; Textile waste; Violet dye; Water treatment.

Highlights:

- *Adsorption performance of corn silk for the crystal violet dye from a simulated aqueous solution.*
- *Solution pH, solution temperature, adsorbent dose, mixing speed, adsorbate concentration, and contact time impact.*
- *The theoretical calculations of adsorption isotherm, kinetics, and thermodynamics.*

ARTICLE INFO

Article history:

Received	16 Nov. 2023
Received in revised form	05 Mar. 2024
Accepted	28 Apr. 2024
Final Proofreading	03 May 2024
Available online	28 May 2025

Citation: Al-Bayati IS, Waisi BI, Mohammed MA, Alobaidy AA, Kadhom MA. **Crystal Violet Dye Removal from Aqueous Solution Using Corn Silks as an Environmentally Friendly Adsorbent**. *Tikrit Journal of Engineering Sciences* 2025; **32**(2): 1876.

http://doi.org/10.25130/tjes.32.2.16

**Corresponding author:*

Basma I. Waisi

Department of Chemical Engineering, College of Engineering, University of Baghdad, Baghdad, Iraq.

Abstract: As today's world faces a crucial water crisis due to increased population and associated development, finding alternative and renewable resources has become necessary. Adsorption is a simple and effective process; when biowaste is applied for this purpose, a reasonable solution is proposed in terms of economical and influential sectors. In the present work, corn silks, usually considered useless, were used to remove the crystal violet dye from a simulated aqueous solution. Different experimental parameters were investigated: solution pH and temperature, adsorbent dose, mixing speed, adsorbate concentration, and contact time. The corn silks were characterized via the SEM microscope, while the chemical functional groups were analyzed using the Fourier transform infrared (FTIR) spectra analysis. The theoretical calculations of adsorption isotherm, kinetics, and thermodynamics were considered to comprehend adsorption nature. The results revealed that as the solution pH reached normality, the highest adsorption removal rate was achieved. After 70 min contact time, the adsorption capacity at a pH of 6.5 was 6.44 mg/g, and the removal rate was 95.5%. Furthermore, the temperature effect test and thermodynamic study showed that the adsorption process was endothermic. However, the adsorption removal rate increased by increasing the adsorbent dose and agitation speed to a certain contact time, and then all became analogous. The dye concentration showed identical behavior, indicating the high adsorption tendency of corn silks. Lastly, the best-fit isotherm and kinetic models were the Freundlich and Pseudo second-order models, respectively.

ازالة الصبغة البنفسجية باستخدام الياف الذرة كمادة مازة صديقة للبيئة

إسراء صبيح البياتي [١]، بسمة إسماعيل ويسي [١]، منال عدنان محمد [١]، اسرار عبدالله العبيدي [١]، محمد عباس كاظم [٢]

[١] قسم الهندسة الكيمياوية / كلية الهندسة / جامعة بغداد / بغداد – العراق.

[٢] قسم علوم البيئة/ كلية علوم البيئة والطاقة/ جامعة الكرخ للعلوم / بغداد – العراق.

الخلاصة

بما أن عالم اليوم يواجه أزمة مياه حادة بسبب الزيادة السكانية والتنمية المرتبطة بها، فقد أصبح من الضروري إيجاد موارد بديلة ومتجددة. الامتزاز تعتبر عملية معالجة بسيطة وفعالة؛ وعندما يتم استخدام المخلفات الحيوية فيها فإنها تمثل حل ذو جدوى فعالة واقتصادية. في هذا البحث، تم استخدام الياف الذرة، والتي تعتبر عادة جزءًا عديم الفائدة، لإزالة الصبغة البنفسجية البلورية من محلول مصنع لمحاكاة المياه الملوثة بالصبغة المذكورة. تم دراسة متغيرات مختلفة وهي: درجة حموضة المحلول، درجة حرارة المحلول، كمية المادة المازة، سرعة الخلط، تركيز المادة الممتزة (الصبغة)، وزمن الخلط. تم تشخيص الياف الذرة باستخدام تقنية الSEM ، في حين تم تحليل المجموعات الوظيفية الكيميائية بواسطة تحليل أطياف الأشعة تحت الحمراء (FTIR). بعدها، تم تطبيق الحسابات النظرية الحركية والديناميكا الحرارية لفهم ميكانيكية الامتزاز. أظهرت النتائج أن أعلى معدل لإزالة يكون في الرقم الهيدروجيني الطبيعي. بعد زمن خلط ٧٠ دقيقة، فأن قدرة الامتزاز عند درجة الحموضة (٦,٥) تكون ٦,٤٤ ملغم/جم معدل الإزالة ٩٥,٥٪. أيضا، أظهر تحليل سلوك درجة الحرارة والدراسة الديناميكية الحرارية أن عملية الامتزاز ماصة للحرارة. من جهة اخرى، فإن معدل إزالة الامتزاز زاد بزيادة كمية المادة الممتزة وسرعة الخلط حتى وقت خلط معين، وبعد ذلك الوقت، يصبح السلوك متماثلا لكل التراكيز. أن أظهار تركيز الصبغة سلوكًا متطابقًا يدل على قابلية الامتزاز العالي الياف الذرة.تم إيجاد ان أفضل الموديلات التي تصف سلوك الأيسوثرم والفعالية الحركية هي نماذج فروندليتش وPseudo second order، على التوالي.

الكلمات الدالة: الامتزاز، حرير الذرة، نفايات النسيج، صبغة بنفسجية، معالجة المياه.

1.INTRODUCTION

The existing fresh water worldwide is continuously depleting as populations and urbanization grow [1]. According to the United Nations World Water Development Report 2021, global wastewater production is estimated to be around 359 billion cubic meters (m^3) per year, of which only 64% is treated. The remaining 36% is released or reused untreated. The ratio of wastewater to freshwater resources varies by country and area; however, it can indicate water stress [2, 3]. The global average wastewater-to-freshwater ratio varies depending on the contaminated water's specification, where for every liter of freshwater used, up to 3 liters of wastewater are generated [4]. Wastewater can pose several problems if not adequately treated [5], leading to health problems for humans and wildlife. Nitrogen and phosphorus are common nutrients in wastewater and can damage aquatic ecosystems through eutrophication. Furthermore, diseases like cholera and typhoid fever can spread due to untreated wastewater [6]. Adsorption is a commonly employed method for eliminating dyes from contaminated water. This method entails binding dye molecules to a solid surface, like activated carbon, clay, or other adsorbent materials [7, 8], through physical or chemical interactions [9]. Adsorption is efficient in purification and separation due to its selective capture, low cost compared to distillation or membrane filtration, and ease of operation with minimal maintenance and simple regeneration. It may be used in many industries, and its environmental friendliness and scalability make it appealing [10, 11]. It is also a versatile technique that could be utilized to remove a wide window of dyes from different types of water [12]. Various studies have reported its effectiveness in adsorbing dyes from textile effluents using different materials and composites [13–15]. Hence, adsorption is applied as a potential solution for treating dye-contaminated. Biowaste is an advantageous and sustainable resource of adsorbents for various contaminating materials. Compared to conventional materials, biowaste offers numerous benefits, such as abundance, low cost, recyclability, and high adsorption capacity. Focusing on dyes, primarily composed of organics [16], various synthesized or grafted biosorbents have been investigated due to their effectiveness in removing dyes [17, 18]. Crystal violet (CV), also known as gentian violet, is commonly studied due to its availability and ease of use. It is a positively charged dye belonging to the triaminoarylmethane family with the chemical formula $C_{25}H_{30}N_3Cl$. This dye is widely utilized in various industries, such as textiles, pharmaceuticals, printing ink, and paper [19]. However, depending on the mode and amount of exposure, it might be dangerous to human health through inhalation, ingestion, or skin contact. Crystal violet has been identified as a potential carcinogen and may cause eye, skin, and digestive tract irritation [20]. From above, biomass represents a valuable source for a wide range of adsorbents that may be used directly or after modification [21]. The modification methods include treating with other materials, preparing biochar, synthesizing activated carbon, and synergizing with other materials [22]. To remove CV, many studies have been published utilizing agricultural waste. For instance, Kristanti et al. [23] studied two adsorbents, i.e., pineapple leaves from the Ananas comosus and lime peels from the Citrus aurantifolia plants, were evaluated at varying quantities (1, 3, 5, 7, and 10 g) to test their effectiveness at removing a 1,000 mg/L solution of CV dye. Lime peels and pineapple leaves eliminated 98% and 97% of CV dye removal. The adsorbents were tested after three hours of incubation. The researchers examined the adsorbent's structure and properties using FESEM and FTIR. Pineapples and lime peels removed 97% and 98% of the dye, respectively. The dye was absorbed because the adsorbent surface was perforated and polymer-containing, according to FESEM. FTIR showed carbonyl and carboxyl groups, aiding adsorption. In another research, Akhtar et al. [24] investigated the effectiveness of Eucalyptus camaldulensis in hindering the CV dye from water. The adsorbent was tested in fixed bed column mode, manipulating the flow rate, bed height, pH, and starting dye concentration. Adsorbent efficacy was assessed using breakthrough curves and exhaust time. At 20 cm bed height, the exhaust time, the most significant breakthrough curve, and mass transfer zone usage were found. The maximum CV content (50 mg/L), low pH (5), and low flow rate (1 mL/min) led to the optimum results. The findings also demonstrated that lower acidic pH improved adsorption capacity and breakthrough curve. Batch-mode adsorption data followed the Langmuir isotherm, and pseudo-second-order reaction kinetics matched well. The breakthrough curve and mass transfer zone were also evaluated and found to meet Thomas's model assumptions. The data matches the Thomas model best with R^2 values (0.933-0.997). The last example uses chemically treated Aloe vera that contains cellulosic moieties to remove the CV dye [25]. The study examined several physicochemical factors, including dosage (0.05-0.5 g), contact time (15-180 min), pH (2-10), temperature (30 - 60°C), and adsorbent initial dye concentration (50-400 mg L^{-1}), and found that these factors significantly influenced the adsorption. The maximum adsorption capacity of CV occurred at pH 9. To analyze the experimental data, adsorption isotherms (Langmuir, Freundlich, and Temkin) and kinetic parameters (pseudo-first-order, pseudo-second-order, and intraparticle diffusion) were applied. The results indicated that the Langmuir isotherm best represented the adsorption of CV onto treated Aloe vera and that the process followed the pseudo-second-order kinetic model. The thermodynamic estimation for enthalpy, free energy, and entropy indicated that the adsorption process was endothermic and spontaneous, and it enhanced the randomness at the adsorbent/adsorbate interface. The presented work studied corn silks as a potentially low-cost, green adsorbent to remove the CV dye. Different parameters were investigated to optimize the operation conditions. The adsorbent was also examined using various techniques to identify the adsorption mechanisms and status. As the used adsorbent is an abundant waste with almost no specified applications, its use for dye removal may present an important sector for its utilization.

2.MATERIALS AND METHODS

2.1.Chemicals

Crystal Violet (CV, $C_{25}H_{30}N_3Cl$) with a 407.99 g/mol molecular weight was purchased from Sigma-Aldrich, MO (USA). Hydrochloric acid (HCl) and sodium hydroxide (NaOH) were obtained from Sigma-Aldrich and used to control the pH of the adsorbate solution. A pH meter (HM Digital waterproof pH-200 meter, Khushkhera, Alwar India PVT. LTD.) was used to measure the pH of the solutions, and deionized (DI) water was used to prepare all aqueous solutions in this study.

The corn silks were collected from the local market in Baghdad, Iraq. The silks were cleaned of dirt and rinsed with water. Then, they were dried at room temperature (25±2 °C) overnight, followed by an oven (Muffle Furnace LMF-F50, Labtron Equipment Ltd., Camberley, United Kingdom) for drying at 70 °C for 12 hours. The dried product was ground in a grinder to cut it into smaller pieces and increase the contact surface area. The final product was placed in a well-closed container to avoid moisture and contamination.

2.2.Dye Solutions Preparation

The adsorbate solutions were prepared by diluting a priorly prepared stock solution of the dye with a concentration of 1000 mg/L. The required specific concentration of the dye solution was prepared by diluting the prepared stock solution of the dye using distilled water. The dye concentrations before and after adsorption were measured using UV-visible spectrophotometers (Thermo Scientific GENESYS 10S Series, Madison, WI, USA) at a wavelength of 598 nm [26]. To adjust the pH of the dye, 0.1 M of NaOH and HCl were utilized, and the pH value was determined using the pH meter.

2.3.Characterization Apparatuses

Field emission scanning electron microscopy (FESEM, JEOL 6335F model, USA) was employed to characterize the silks' surface morphology. To track changes in the surface functional groups, Fourier transform infrared (FTIR) analysis was conducted before and after adsorption using the Nicolet iS10 FTIR instrument (Thermo Fisher Scientific Inc., Waltham, MA, USA). The surface area of the used corn silk was analyzed by N2 adsorption using the Brunauer–Emmett–Teller (BET) analyzer (CET Scientific Services (CET), Singapore).

2.4.Adsorption Studying Conditions

In this work, a batch system was used to investigate the equilibrium analysis; several factors were examined to understand their impact on the adsorption process. These factors included the initial dye concentration ranging from 10 to 40 mg/L, solution pH ranging from 4.5 to 9, and adsorbent dose from 0.2 to 1.2 g. Furthermore, rotating speeds of 100 to 300 rpm and temperatures from 15 to 35 °C were considered. The effect of the mentioned factors was studied in a time range of 0-70 min. Except for the mixing speed examination, all samples were placed in a shaker (BSG-10 Orbital Shaker, Jiangsu, China) and subjected to a constant oscillation of 200 rpm. To adjust the pH of the solution, diluted HCl or NaOH (0.1 M) was utilized. The data were collected at different intervals before equilibrium was achieved and during the adsorption process. The dye concentration was determined using a UV-Vis spectrophotometer.

2.5.Isotherm Study

The equilibrium adsorption of the CV under optimal conditions and at different temperatures was analyzed using Langmuir and Freundlich isotherms, as described by Eqs. (1) and (2) [9], respectively:

$$\frac{C_e}{q_e} = \frac{1}{K_L q_{max}} + \frac{C_e}{q_m} \quad (1)$$

$$lnq_e = lnK_F + \frac{1}{n} * lnC_e \quad (2)$$

where C_e represents the equilibrium concentration of the dye (mg/L). q_e (mg/g) and q_m (mg/g) represent the equilibrium dye and the Langmuir maximum uptakes, respectively. K_L indicates the Langmuir constant (L/mg), K_F (mg/g) is the Freundlich adsorption capacity, and n represents the surface heterogeneity constant. Based on the Langmuir model, the adsorption process involves the monolayer coverage on a homogeneous adsorbent surface. The surface contains a finite number of identical adsorption sites with similar adsorption energies. On the other hand, the Freundlich isotherm suggests a heterogeneous adsorbent surface with non-identical vacant sites. It also assumes a non-uniform heat distribution over the multilayer coverage [1,27].

2.6.Kinetic Study

Adsorption kinetics plays a crucial role in understanding the reaction pathways and interaction mechanisms between the silks and the CV. In this study, the kinetic conductance of the dye was investigated at various concentrations (ranging from 10 to 40 mg/L) under optimum conditions, which included neutral pH (7), 200 rpm agitation speed, 20 mg/L dye concentration, 25 °C, and 0.6 g silks powder. The investigation involved using linear equations derived from the pseudo-first-order and pseudo-second-order models. The pseudo-first-order kinetic model proposes that the rate of adsorption is proportional to the number of available sites while also considering a physical interaction between the adsorbate and the adsorbent [27]. However, the pseudo-second-order kinetic model suggests that chemisorption or chemical bonding between the adsorbent and adsorbate affects adsorption. This model suggests that the adsorbent and adsorbate exchange electrons to form a more stable adsorption configuration. Unlike the pseudo-first-order model, the pseudo-second-order model accounts for occupied and unoccupied sites on the adsorbent surface and is affected by adsorbate concentration [28]. The pseudo-first- and -second-order models are represented in Eqs. (3) and (4) [28], respectively.

$$\log(q_e - q_t) = logq_e - \frac{K_1}{2.303} * t \quad (3)$$

where t (min) represents the time. q_e and q_t (mg/g) denote the dye uptake at equilibrium and at a specific time, respectively. K_1 (min^{-1}) represents the pseudo-first-order constant.

$$\frac{t}{q_t} = \frac{1}{K_2 * q_e^2} + \frac{t}{q_e} \quad (4)$$

where q_e and q_t (mg/g) are the adsorption capacities at equilibrium and at any given time, respectively. The time variable, t, is measured in minutes, and K_2 represents the pseudo-second-order constant (g/mg min).

2.7.Thermodynamic Study

To assess the influence of temperature on the adsorption process, the thermodynamic parameters were analysed. The Van't Hoff equation was used to calculate the standard enthalpy change (ΔH°), Gibbs free energy change (ΔG°), and standard entropy change (ΔS°) values, as below [29]:

$$\Delta G^o = -RTlnK \quad (5)$$

$$\Delta G^o = \Delta H^o - T\Delta S^o \quad (6)$$

$$lnK = \frac{-\Delta H^o}{RT} + \frac{\Delta S^o}{R} \quad (7)$$

$$K = \frac{C_{Ae}}{C_{Se}} \quad (8)$$

where T is the temperature (°C), K is the equilibrium constant, and R is the gas constant (8.314 J/molK). C_{Ae} and C_{Se} denote the dye concentrations in equilibrium on the silks (mg/L) and in the solution (mg/L), respectively. The Arrhenius equation [30] can be used to estimate the activation energy (E), as shown below:

$$lnK_2 = lnA - \frac{E}{RT} \quad (9)$$

where E represents the activation energy in J/mol, K_2 is the pseudo-second-order constant, and A is the Arrhenius constant in g/mol.

3.RESULTS AND DISCUSSION

3.1.Adsorbent Characterization

Figure 1 shows SEM images of the absorbent silks. The images indicate that each corn silk fiber was elongated in style with tiny ripples. The SEM images demonstrate the tubular, hole- and void-filled structure of corn silk, which aids in the adsorption and adherence of contaminants on the surface of the material due to the high contact surface of the adsorbent. The diameter of the tubular construction, filled with holes and spaces, ranged from 5 to 20 µm. These dimensions demonstrate the existence of macroporous structure, explaining why maize silk has a low bulk density. Therefore, the porosity of the internal fiber and surface configuration work together to improve sorption.

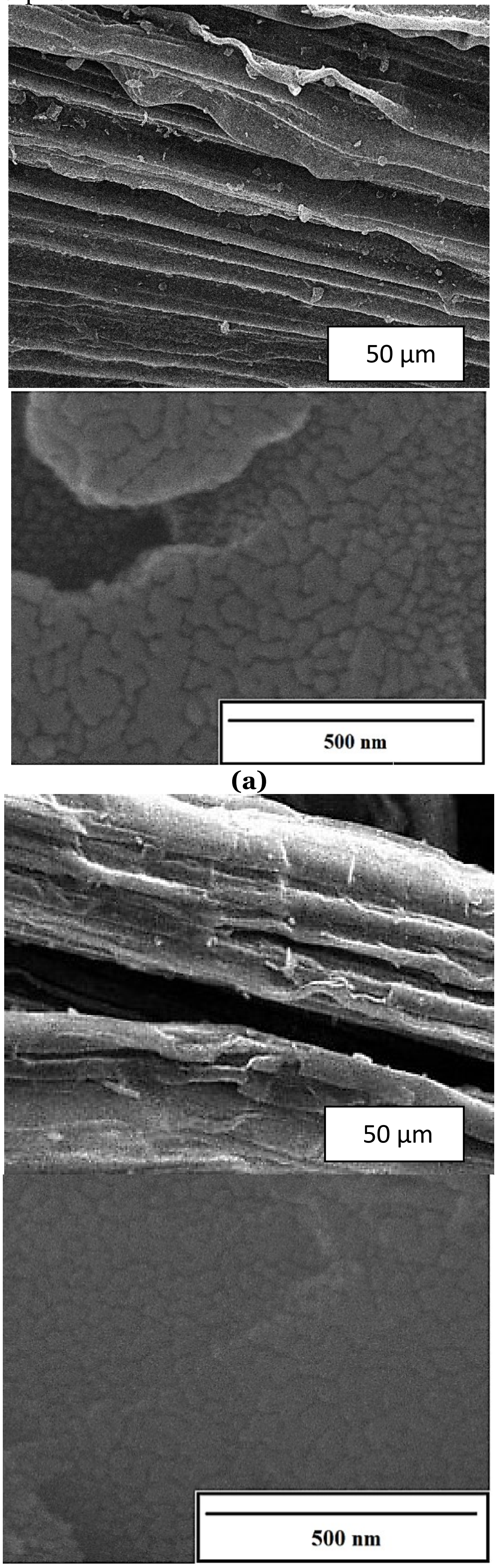

(b)

Fig. 1 Different SEM Surface Morphology Images of the Corn Silks (a) before and (b) after Dye Adsorption.

FTIR analysis was conducted to identify the functional groups on the surface of the adsorbent. In Fig. 2 (a) and (b), the FTIR spectra before and after adsorption are depicted, respectively. The wavelength studied ranged from 4000 to 400 cm^{-1}, and many peaks were indicated for the adsorbent material. Corn fibers are mainly comprised of lignin, cellulose, hemicelluloses, and tannins. The peak value at 3445 cm-1 corresponds to the hydroxyl group (-OH) of the phenolic group in cellulose, hemicellulose, lignin, and absorbed water. The 2890-2930 cm^{-1} peak corresponds to the stretching and bending vibration of -CH groups in methyl and methylene groups found in cellulose and hemicellulose. The peak found at 1730 cm^{-1} is attributed to the stretching of the –CO bond in phenols and carboxylic acids. Abundant carboxyl and hydroxyl groups may coordinate with positive ions of cationic dyes. Peaks between 1500 and 1600 cm–1 suggest the existence of lignin in the natural fiber. The intense C-O stretching signals were seen between 1027 and 1037 cm^{-1}, attributed to lignocellulosic materials. The functional collections following the adsorption process of CV dyes were marginally affected by location and density, ascribing to interactions between the nitrogen atoms in the dye's amine groups and the surface functional groups (hydroxyl and carboxyl groups) [31].

3.2.Studying Different Parameters Effect

The effect of physical parameters, namely pH, adsorbent dose, agitation speed, dye's initial concentration, and solution temperature, on the removal rate was studied. Below is the detailed experimental investigation.

3.2.1.pH Effect

The impact of pH within the range of 4.5 to 9.5 on dye removal was examined to comprehend its influence, as it is a critical factor that influences the adsorbate and adsorbent. Changes in pH can affect dye adsorption by modifying the surface charge of the adsorbent as well as the dissociation of dyes within the solution. Hence, investigating this parameter was considered to ascertain the pH's effect on the substance being adsorbed, excluding using an adsorbent. Various solutions of different pHs were prepared, while other parameters were fixed. The solutions contained dye at a concentration of 20 mg/L and were mixed at 200 rpm and room temperature, while 0.6 g of the adsorbent was used. The initial and final pH values were measured at 598 nm. Notably, a change in the removal rates was noticed as pH values were changing, which could be attributed to the pH's influence on the chemical structure of the dye and consequently affecting its color intensity [32]. Figure 3 shows the effect of the solution's pH on the removal rate at a contact time range of 0-90 min. From the figure, the removal rate enhanced as the contact time increased at all pH values. By focusing on the pH, it can be seen that the lowest removal was obtained at pH=4.5, indicating the bad effect of the acidic media. This behavior could be comprehended by considering the presented charge on the adsorbent surface. When the solution's pH is low, the positive charge is dominated. As a result, there is an electrostatic repulsion between the cationic dye and the positively charged ions within the solution [33]. The highest removal rate was achieved at a pH = 6.5. Then, a reduction occurred at higher pHs. This decrease could be attributed to the loss of hydrogen ions that CV molecules could undergo and become deprotonated. Hence, the dye molecule acquires a negative charge, and its attraction to negatively charged surfaces will be diminished. The negatively charged dye molecules reject surfaces; neither are adsorbed nor absorbed [34, 35]. Thereby, the dye removal conditions are optimized at neutral or nearly neutral pHs due to the ability to mitigate the repulsive interactions generated by charges that reduce the interactions between dye molecules and surfaces. It is worth noting that the adsorption process was fast, and at the pH of 6.5, it only took 10 min to achieve more than 90% of the equilibrium capacity. Furthermore, the adsorption capacity at pH of 6.5 and 70 min was 6.44 mg/g.

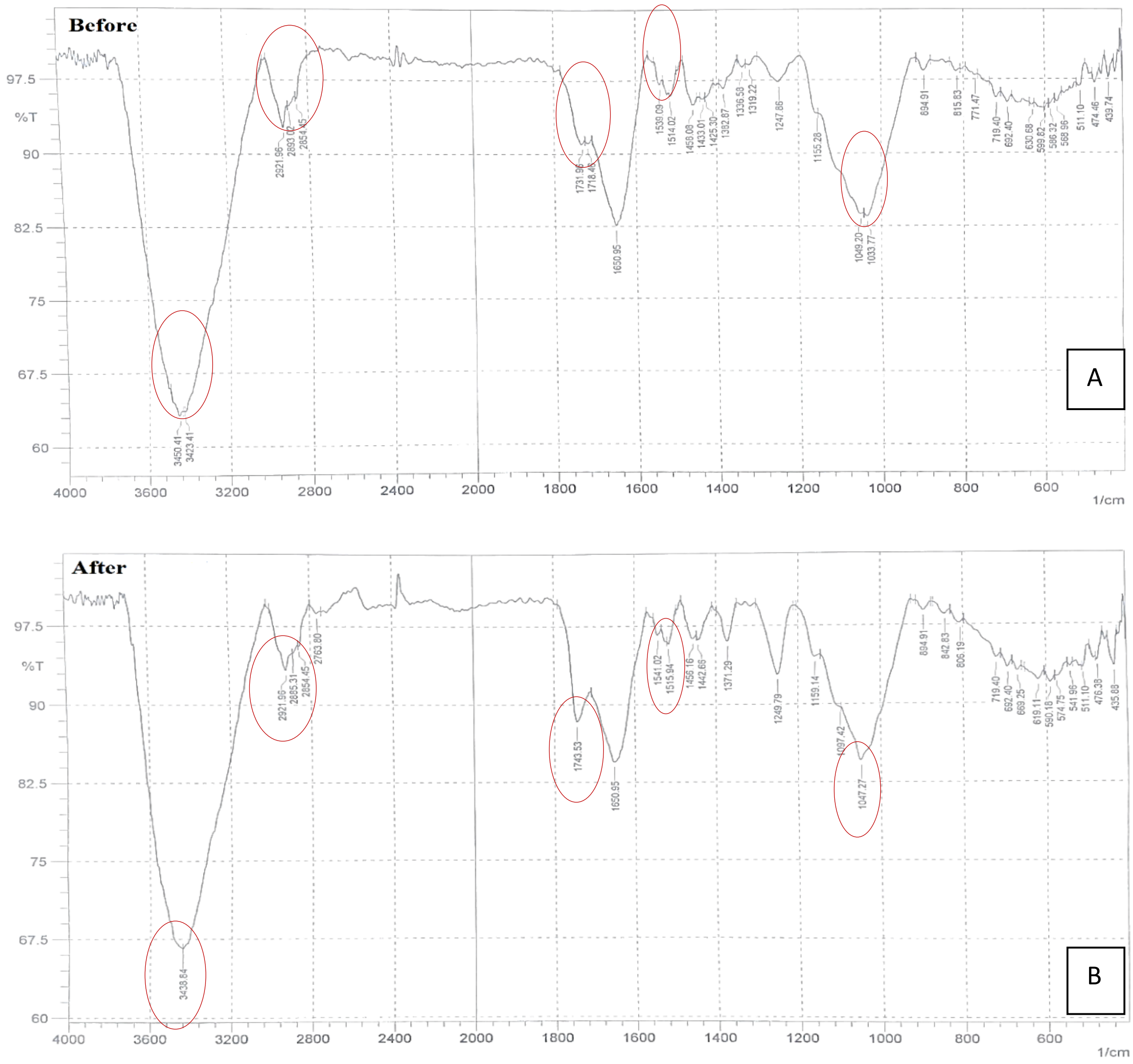

Fig. 2 FTIR Test for the Adsorbent: (a) before Adsorption of CV Dye and (b) after Adsorption.

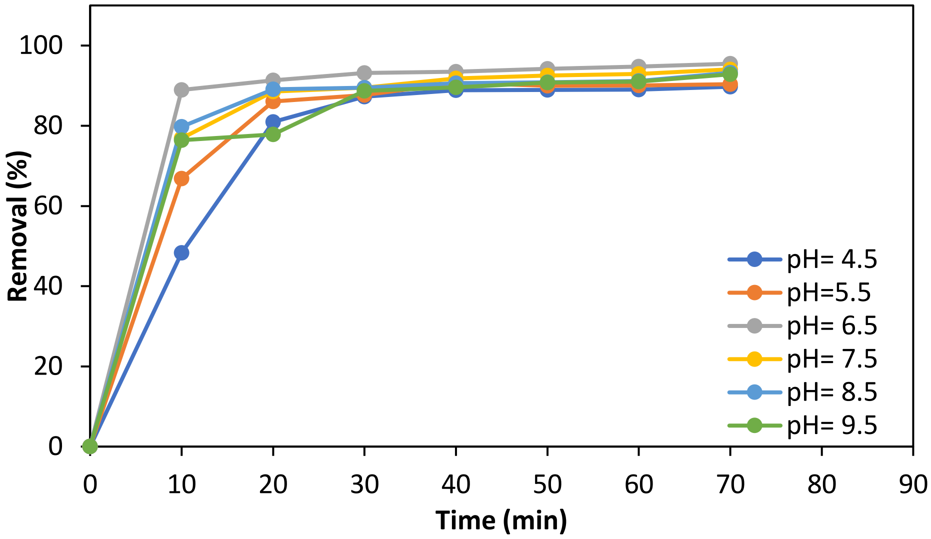

Fig. 3 pH Impact on Removal Rate at Different Contact Time Intervals, at Adsorbent Dose =0.6 g, Agitation Speed = 200 rpm, and Initial Dye Concentration = 20 mg/L.

3.2.2. *Effect of the Adsorbent Dose*

To investigate the impact of the adsorbent on adsorption, varying doses of corn silks (0.2 – 1.2 g) were employed at room temperature with a dye concentration of 20 mg/L and container volume of 50 ml. As depicted in Fig. 4 and at low contact time, the removal dosage impact was clear, where the highest dosage (1.2 g) showed 94.85 % removal compared with the lowest (0.2 g), which showed 78.72 % removal at 10 min contact time. This rise was attributed to the availability of additional unoccupied sites at a fixed concentration, promoting easier accessibility and a larger surface area [36]. However, the effectiveness of dye removal exhibited an enhancement, ranging from 80 % to 96.3 %, with an increase in silk dose from 0.2 g to 1.2 g after one hour of contact. At high doses, potential interactions between adsorbents might reduce capacity due to agglomeration and aggregation, resulting in a diminished overall surface area [37]. According to the results, the optimum dose of corn silks was 0.6 g, as no noticeable effect on the removal percentage was observed at the higher amount of adsorbent.

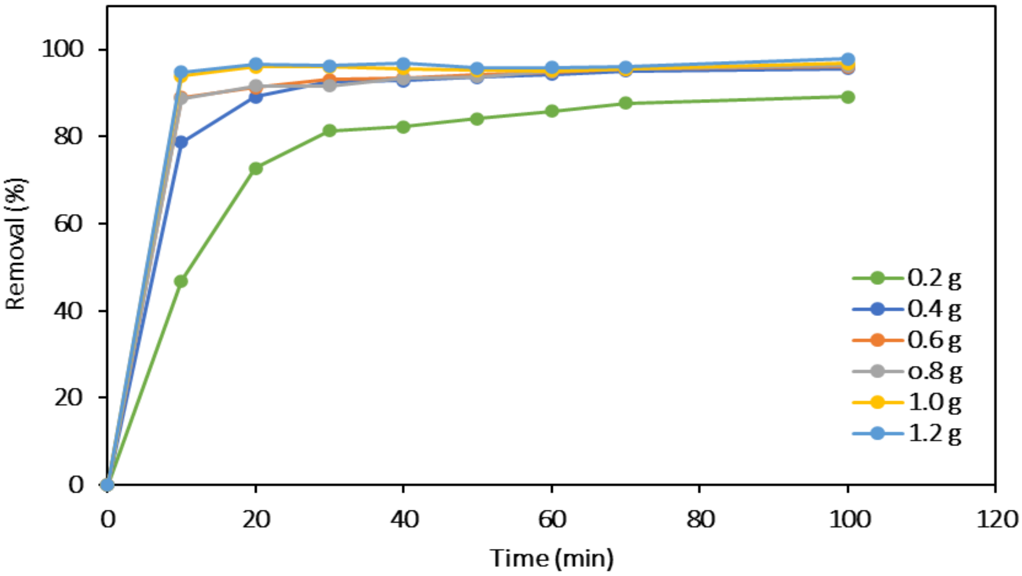

Fig. 4 Effect of Adsorbent Dose on the Removal Rate at pH= 6.5, Agitation Speed = 200 rpm, and Initial Dye Concentration = 20 mg/L.

3.2.3. *Impact of Agitation Speed*

Mixing is significant in the process of adsorption due to its influence on the interaction between the adsorbent and adsorbate. Thus, the optimal mixing speed at pH=6.5 and adsorbent dose= 0.6 g fell within the range of 100 to 300 rpm, which was employed as depicted in Fig. 5. At short contact time intervals, the outcomes demonstrated an initial rise in the removal percentage with higher mixing rates, indicating an enhanced adsorption process initiation. Yet, the difference between 200 and 300 rpm agitation was marginal, which could be explained as elevated mixing speeds contributing to improved adsorption by thinning the boundary layer, thereby facilitating increased film diffusion. Additionally, mixing facilitates the even spread and distribution of adsorption particles across the silk's surface [38]. Nonetheless, further elevation of mixing speed might not continue to enhance adsorption, eliminating external diffusion impact [39]. This behavior is observed in the figure as the contact time achieves 50 min, where all studied mixing speeds showed identical curves. The optimum agitation speed was 200 rpm as the removal percentage remained stable at a further mixing rate.

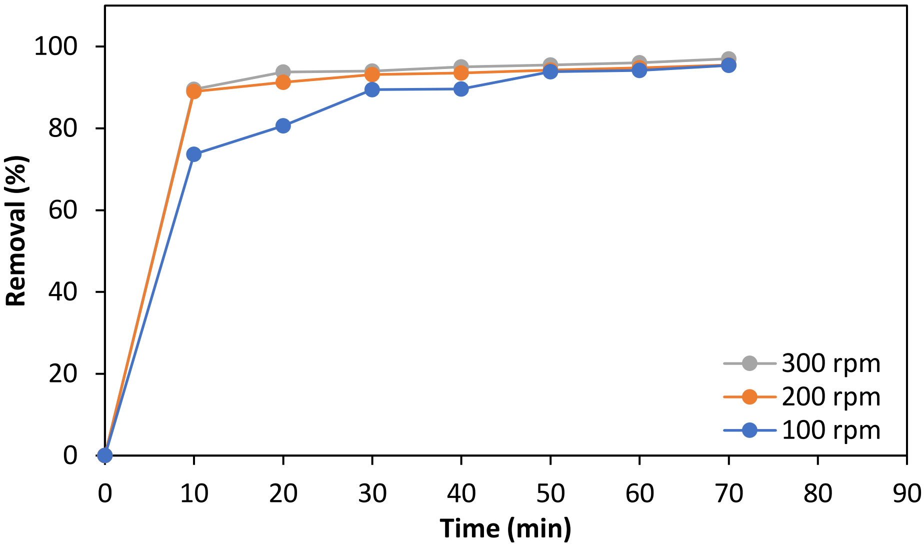

Fig. 5 Effect of Agitation Speed on Removal Rate at pH= 6.5, Adsorbent Dose of 0.6 g, and Initial Dye Concentration = 20 mg/L.

3.2.4.Impact of Dye's Initial Concentration

The initial dye concentration plays a pivotal role in the adsorption process as the sorbent material's capacity to absorb dye is fixed. Hence, the adsorption process is contingent on the concentration of the dye. In the present study, a dye solution ranging from 10 to 40 mg/L was utilized alongside 0.6 g of corn silks, maintaining a neutral pH of 6.5 and room temperature. The outcomes in Fig. 6 reveal that the dye removal marginally escalated as the concentration decreased. Other studies indicated that low initial dye concentrations experience better results as ample vacant binding sites are available, which promotes effective and swift adsorption. Moreover, dye molecules at higher concentrations might compete for these sites, leading to saturation and reduced removal [39]. Conversely, elevated dye concentrations can enhance adsorption capacity due to the heightened driving force that surpasses mass transfer resistance [40]. However, in the present study, the removal ratios were identical at all initial concentrations, indicating the high adsorption capability of the used material. From the figure, the adsorption was almost completed in the first 10 min, and the equilibrium was achieved after that, which could be comprehended as vacant binding sites on the silks were accessible for dye uptake; however, with time, the adsorption rate decelerated as these sites became progressively occupied [41].

3.2.5.Impact of Solution Temperature

The impact of solution temperature on the removal rate was examined using three distinct temperatures: 15, 25, and 35 °C at the optimum values of other parameters (pH= 6.5, adsorbent dose= 0.6 g, agitation speed= 200 rpm, and initial dye concentration= 20 mg/L). The influence of these temperatures is illustrated in Fig. 7 across varying contact durations within the range of 0-70 minutes. As observed from Fig. 7, the removal rate gradually increased at 15 °C, ultimately reaching its peak after 70 minutes. Conversely, at 25 °C, equilibrium was attained faster, whereas at 35 °C, the escalation was even more rapid. These observations suggest an endothermic nature of the process, predominantly characterized by physical adsorption facilitated by the presence of pores and internal cracks within the corn silk structure. This phenomenon implies that elevated temperatures of the aqueous contribute to reinforcing interaction forces between the adsorbate and adsorbent [42].

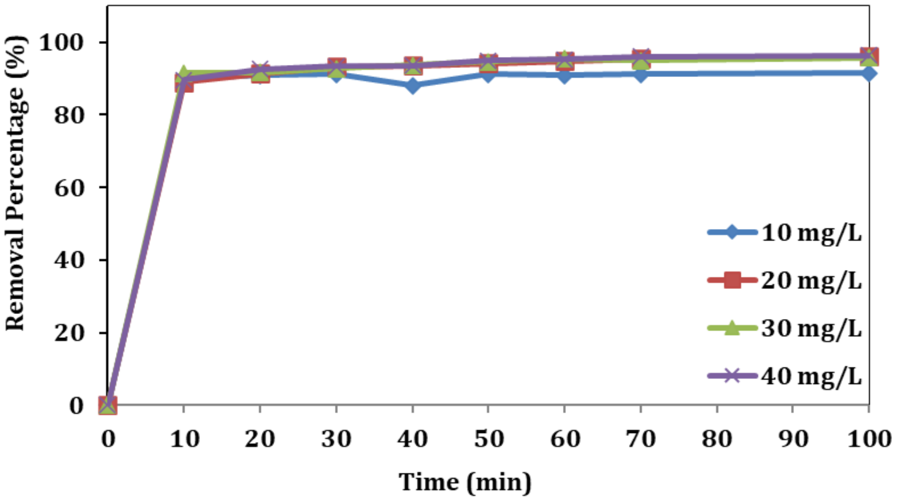

Fig. 6 Effect of Dye's Concentration on the Removal Rate at pH=6.5, Adsorbent Dose=0.6 g, and Agitation Speed=200 rpm.

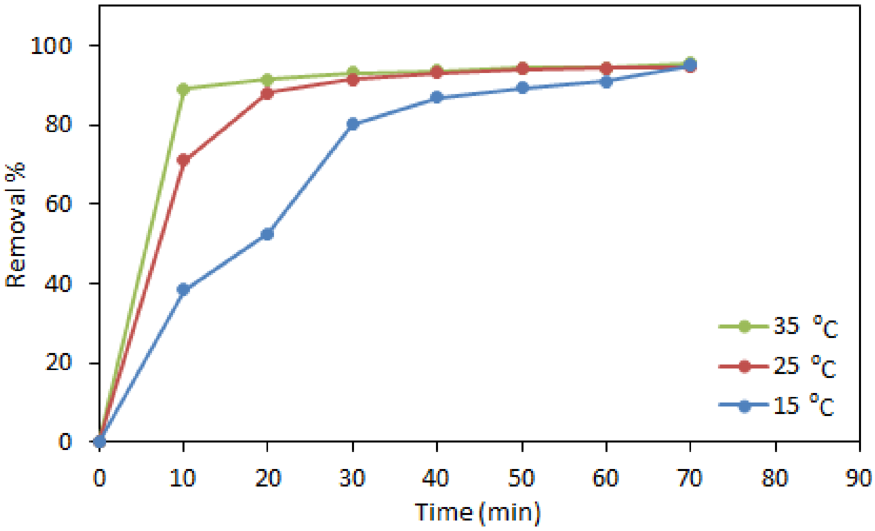

Fig. 7 Impact of Temperature on the Removal Rate (pH= 6.5, Adsorbent Dose= 0.6 g, Agitation Speed= 200 rpm, and Initial Dye Concentration= 20 mg/l).

3.3.Isothermal, Kinetic, and Thermodynamic Studies

3.3.1. Isotherm Study

In this section, two models were investigated, namely Langmuir and Freundlich, which are commonly used for this purpose. The correlations were plotted as illustrated in Fig. 8 to clarify their proportion. Table 1 shows the model variables, and regression analysis was used to measure the linear model's correlation with the dependent variables as a percentage from 0 to 100%. From these figures, the maximum adsorption capacity was achieved via the Freundlich model. Furthermore, by assessing the correlation factor (R^2), the most suitable isotherm model could be identified. The data indicated that the Freundlich model exhibited the best fit, which is evident from the higher R^2 values, indicating the multilayer adsorption mode occurring on a heterogeneous surface. The Freundlich model suggests that adsorption occurs on surfaces with variations in the interaction strength between the molecules and the surface. This type of adsorption is not constrained to a single-layer formation and is especially valuable for describing multiple layers of adsorbate on irregular morphology [43, 44].

Table 1 Isotherm Models Information.

Langmuir				Freundlich		
q_{max} (mg/g)	K_L (L/mg)	R^2	R_L	K_F ($mg^{1-n} g^{-1} L^n$)	n	R^2
1.73	1.39	0.98	0.08	9.9686	0.207	0.992

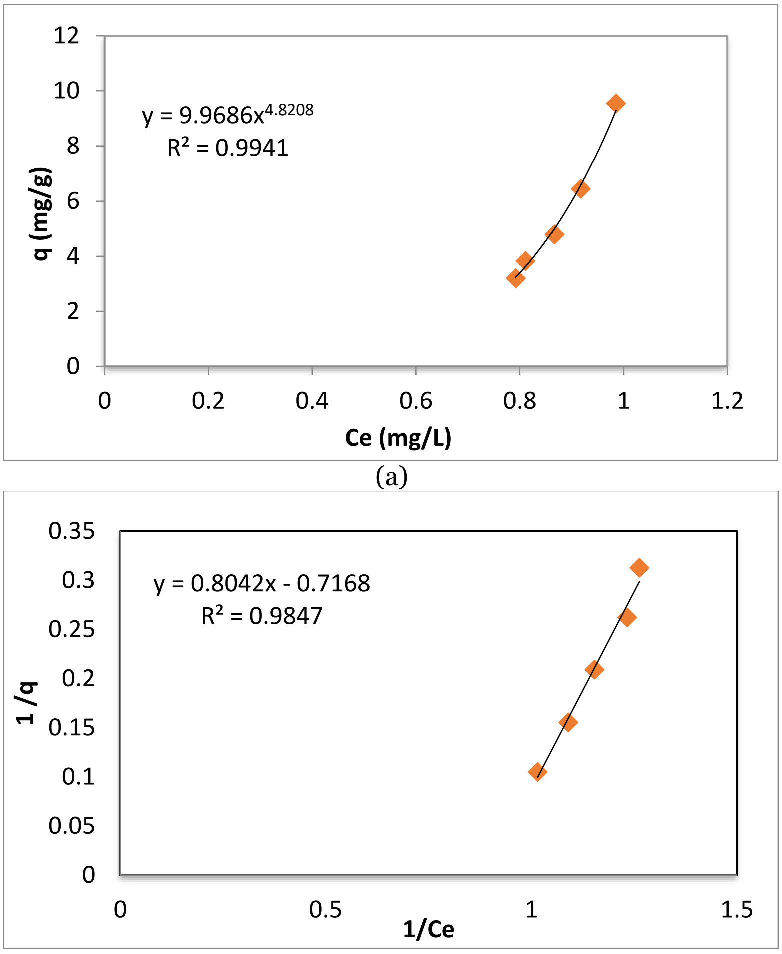

(a)

(b)

Fig. 8 Adsorption Isotherms: (a) Langmuir and (b) Freundlich Models.

3.3.2.Kinetic Study

In this part, and among the different studying models, the two most familiar ones were selected, the Pseudo-first- and second-order models. The physisorption-constrained adsorption rate of particles onto the adsorbent is the focus of the pseudo-first-order model, whereas the pseudo-second-order model attributes the process's rate-limiting step to chemisorption [45]. Table 2 shows the calculated values of the two models, and Fig. 9 shows their plotting considering R^2 values. From Fig. 9, it can be inferred that the Pseudo-second-order model fits better than the first-order one, pointing to a chemical interaction between the dye and the silks. The computed uptake values closely matched the real uptake values, with R^2 values approaching unity. A similar behavior was reported for the CV dye when orange peels were employed for the same purpose [46].

Table 2 Kinetic Study Parameters.

$q_{e\,exp}$ mg/g	Pseudo first order			Pseudo second order		
	$q_{e\,cal}$ (mg/g)	k_1 (min^{-1})	R^2	$q_{e\,cal}$ (mg/g)	k_2 (g/min mg)	R^2
6.44	0.102	-5.5	0.8176	6.49	0.24	0.999

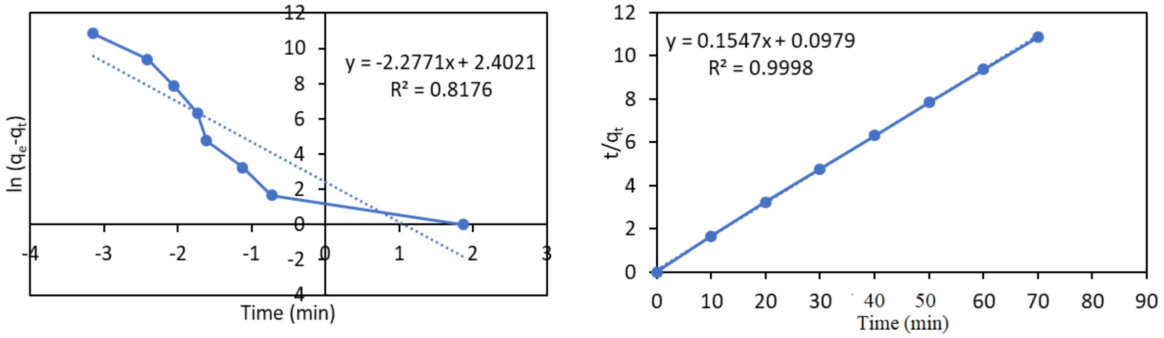

(a) (b)

Fig. 9 Kinetic Study Models: (a) Pseudo First Order and (b) Pseudo Second Order.

3.3.3.Thermodynamic Study

The alteration in standard enthalpy (ΔH^o) and standard entropy (ΔS^o) was determined by analyzing the slope and the point of intersection in the Van't Hoff equation, the outcomes of which are presented in Table 3 and Fig. 10. The activation energy value can be derived from the graphical representation of $\ln K_c$ against 1/T. This parameter shows the type of adsorption and the interaction between molecules and the adsorbent. The values in Table 3 demonstrate negative Gibbs free energy, indicating a spontaneous adsorption process. However, as the temperature increased to 25 °C, the ΔG^o decreased, while the value increased when the temperature was 35 °C. At higher temperatures, molecular mobility increased, suggesting favorable adsorption conditions at elevated temperatures [47, 48]. On the other hand, the positive enthalpy value indicates an endothermic process, which supports the findings related to the temperature effect in Fig. 7. Simultaneously, the positive entropy value indicates an enhancement in randomness at the interface [49,50].

Table 3 Thermodynamic Parameters.

T (°C)	k_c	ΔG^o (J/mol)	ln kc	1/T	ΔH^o (J/mol)	ΔS^o (J/mol.K)
15	5.277778	-25735.3	1.663505	0.003472	10899.65	51.51271
25	5.789007	-26250.4	1.755961	0.003356		
35	7.102564	-14835.7	1.960456	0.003247		

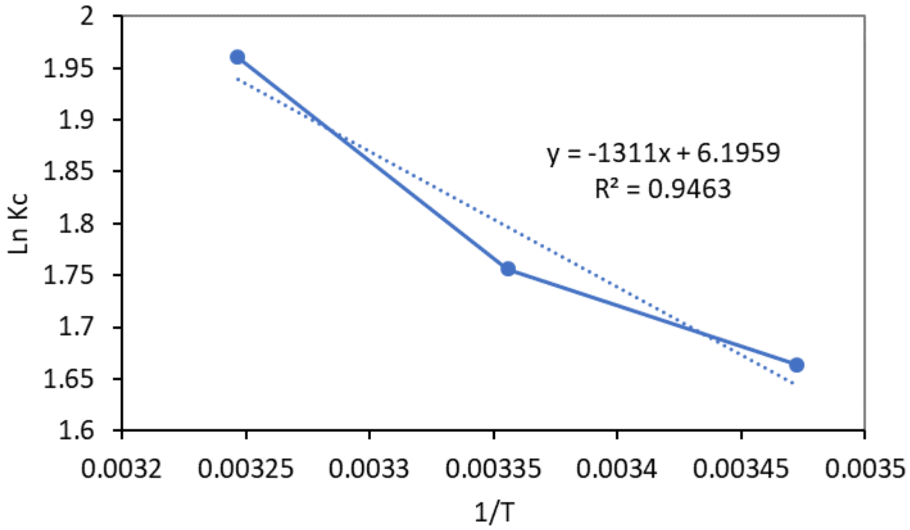

Fig. 10 Thermal Study Based on Van't Hoff Equation.

4.CONCLUSIONS

The present study investigated adsorption, a straightforward yet potent process that can catalyze economic and influential transformations. By employing corn silks as a harnessed biowaste and inconsequential remnants, the crystal violet dye from aqueous water could be separated. A rigorous exploration of multiple experimental variables encompassing solution pH, adsorbent dosage, adsorbate concentration, mixing speed, contact time, and temperature unveiled a comprehensive understanding of the adsorption phenomenon. The adsorption was confirmed by employing SEM images to visualize the corn silks and FTIR spectra analysis to elucidate the dye. The theoretical analyses of adsorption isotherms, kinetics, and thermodynamics were engaged. Through examination, the present findings illuminated the pivotal role of normalizing solution pH in achieving maximal adsorption rates. Notably, at a pH of 6.5 and after 70 minutes, an adsorption capacity of 6.44 mg/g was attained, accompanied by a remarkable removal rate of 95.5%. Interestingly, increasing adsorbent dosage and agitation speeded up to a certain contact time increased adsorption removal rates, reaching equilibrium. Dye concentration followed this trend, confirming corn silks' remarkable adsorption ability. The Freundlich and Pseudo-second-order models best fit the experimental data. In addition, temperature behavior tests and thermodynamic studies illustrated the endothermic nature of adsorption. This study illuminates biowaste's untapped potential for mitigating waterborne pollutants and emphasizes the need to use such unconventional resources to solve the global water crisis. Further studies on developing carbon-based materials from corn silks and the economic analysis of using biowaste are recommended.

ACKNOWLEDGMENTS

The authors thank the Department of Chemical Engineering at the University of Baghdad for partially supporting this work.

FUNDING

None

CONFLICT OF INTEREST

The authors declare no known conflict in this work.

REFERENCES

[1] Salih SS, Mahdi A, Kadhom M, Ghosh TK. **Competitive Adsorption of as (III) and as (V) onto Chitosan/Diatomaceous Earth Adsorbent.** *Journal of Environmental Chemical Engineering* 2019; **7**(5):103407.

[2] Al-Furaiji MH, Karim UF, Augustijn DC, Waisi BI, Hulscher SJ. **Evaluation of Water Demand and Supply in the South of Iraq.** *Journal of Water Reuse and Desalination* 2016; **6**(1):214-226.

[3] Jones ER, Van Vliet MT, Qadir M, Bierkens MF. **Country-Level and Gridded Estimates of Wastewater Production, Collection, Treatment and Reuse.** *Earth System Science Data* 2021; **13**(2):237-254.

[4] Waisi BI, Karim UF, Augustijn DC, Al-Furaiji MH, Hulscher SJ. **A Study on the Quantities and Potential Use of Produced Water in Southern Iraq.** *Water Science and Technology: Water Supply* 2015; **15**(2):370-376.

[5] Mohammed MA, Al-Bayati IS, Alobaidy AA, Waisi BI, Majeed N. **Investigation the Efficiency of Emulsion Liquid Membrane Process for Malachite Green Dye Separation from Water.** *Desalination and Water Treatment* 2023; **307**(9):190-195.

[6] Salih SS, Kadhom M, Shihab MA, Ghosh TK. **Competitive Adsorption of Pb (II) and Phenol onto Modified Chitosan/Vermiculite Adsorbents.** *Journal of Polymers and the Environment* 2022; **30**(10):4238-4251.

[7] Mahmood OA, Waisi BI. **Synthesis and Characterization of Polyacrylonitrile Based Precursor Beads for the Removal of the Dye Malachite Green from its Aqueous Solutions.** *Desalination and Water Treatment* 2021; **216**:445-455.

[8] Mahmood OA, Waisi BI. **Crystal Violet Dye Removal from Aqueous Water Using Polyacrylonitrile Precursor Beads.** *Materials Today: Proceedings* 2021; **42**:2185-2192.

[9] Kadhom M, Kalash K, Al-Furaiji M. **Performance of 2D MXene as an Adsorbent for Malachite Green Removal.** *Chemosphere* 2022; **290**:133256.

[10] Kalash KR, Al-Furaiji MH, Waisi BI, Ali RA. **Evaluation of Adsorption Performance of Phenol Using Non-Calcined Mobil Composition of Matter No. 41 Particles.** *Desalination and Water Treatment* 2020; **198**:232-240.

[11] Hussein BI. **Removal of Copper Ions from Waste Water by Adsorption with Modified and Unmodified Sunflower Stalks.** *Journal of Engineering* 2010; **16**(3):5411-5421.

[12] Salih SS, Mohammed HN, Abdullah GH, Kadhom M, Ghosh TK. **Simultaneous Removal of Cu (II), Cd (II), and Industrial Dye onto a Composite Chitosan Biosorbent.** *Journal of Polymers and the Environment* 2020; **28**:354-365.

[13] Al-Bayati IS, Mohammed SA, Al-Anssari S. **Recovery of Methyl Orange from Aqueous Solutions by Bulk Liquid Membrane Process Facilitated with Anionic Carrier.** *AIP Conference Proceedings* 2023; **2414**(1): 060010.

[14] Waisi BI, Al-Furaiji MH, McCutcheon JR. **Activated Carbon Nanofibers Nonwoven Flat Sheet for Methylene Blue Dye Adsorption: Batch and Flow-Through Systems.** *Desalination and Water Treatment* 2023; **289**:228-237.

[15] Mohammed MA, Noori WO, Sabbar HA. **Application of Emulsion Liquid Membrane Process for Cationic Dye Extraction.** *Iraqi Journal of Chemical and Petroleum Engineering* 2020; **21**(3):39-44.

[16] Kadhom M, Albayati N, Alalwan H, Al-Furaiji M. **Removal of Dyes by Agricultural Waste.** *Sustainable Chemistry and Pharmacy* 2020; **16**:100259.

[17] Elgarahy AM, Elwakeel KZ, Mohammad SH, Elshoubaky GA. **A Critical Review of Biosorption of Dyes, Heavy Metals and Metalloids from Wastewater as an Efficient and Green Process.** *Cleaner Engineering and Technology* 2021; **4**:100209.

[18] Adil H, Hussain Z, Kadhom M, Yousif E. **Adsorptive Removal of Safranin-O Dye from Aqueous Solutions Using Carrot Seed.** *AIP Conference Proceedings* 2022; **2394**(1): 040011, (1-8).

[19] Abbasi AR, Karimi M, Daasbjerg K. **Efficient Removal of Crystal Violet and Methylene Blue from Wastewater by Ultrasound Nanoparticles Cu-MOF in Comparison with Mechanosynthesis Method.** *Ultrasonics Sonochemistry* 2017; **37**:182-191.

[20] Muthukumaran C, Sivakumar VM, Thirumarimurugan M. **Adsorption Isotherms and Kinetic Studies of**

Crystal Violet Dye Removal from Aqueous Solution Using Surfactant Modified Magnetic Nanoadsorbent. *Journal of the Taiwan Institute of Chemical Engineers* 2016; **63**:354-362.

[21] Hussein TK, Jasim NA. **Removal of Crystal Violet and Methylene Blue from Synthetic Industrial Wastewater Using Fennel Seed as an Adsorbent.** *Journal of Engineering Science and Technology* 2019; **14**(5):2947-2963.

[22] Alalwan HA, Kadhom MA, Alminshid AH. **Removal of Heavy Metals from Wastewater Using Agricultural Byproducts.** *Journal of Water Supply: Research and Technology—AQUA* 2020; **69**(2):99-112.

[23] Kristanti RA, Yuniarto A, Hadibarata T. **Adsorption of Basic Dyes Crystal Violet on Agricultural Biomass: Characterization, Isotherm, and Kinetic Studies.** *International Journal of Integrated Engineering* 2022; **14**(1):269-275.

[24] Akhtar M, Khan SU, Mazhar N, Naveed M, Muhammad Q. **Optimization of Crystal Violet Dye Removal in Fixed Bed Column Using *Eucalyptus camaldulensis* as a Low-Cost Adsorbent.** *Letters in Applied NanoBioScience* 2022; **11**(4):4114-4130.

[25] Ahmad A, Lokhat D, Rafatullah M, Khatoon A, Setapar SH. **Aloe Vera Biomass Containing Cellulosic Moieties Used as Sustainable Adsorbents for the Removal of Crystal Violet Dye from Aqueous Solution.** *Desalination and Water Treatment* 2019; **170**:337-348.

[26] Aref L, Navarchian AH, Dadkhah D. **Adsorption of Crystal Violet Dye from Aqueous Solution by Poly (Acrylamide -Co- Maleic Acid) /Montmorillonite Nanocomposite.** *Journal of Polymers and the Environment* 2017; **25**:628-639.

[27] Brião GV, Jahn SL, Foletto EL, Dotto GL. **Adsorption of Crystal Violet Dye onto a Mesoporous ZSM-5 Zeolite Synthetized Using Chitin as Template.** *Journal of Colloid and Interface Science* 2017; **508**:313-322.

[28]

[29] Ebelegi AN, Ayawei N, Wankasi D. **Interpretation of Adsorption Thermodynamics and Kinetics.** *Open Journal of Physical Chemistry* 2020; **10**(3):166-182.

[30] Du C, Song Y, Shi S, Jiang B, Yang J, Xiao S. **Preparation and Characterization of a Novel Fe3O4-Graphene-Biochar Composite for Crystal Violet Adsorption.** *Science of the Total Environment* 2020; **711**:134662.

[31] Salih SS, Kadhom M, Shihab MA, Ghosh TK. **Competitive Adsorption of Pb (II) and Phenol onto Modified Chitosan/Vermiculite Adsorbents.** *Journal of Polymers and the Environment* 2022; **30**(10):4238-4251.

[32] Cheriaa J, Khaireddine M, Rouabhia M, Bakhrouf A. **Removal of Triphenylmethane Dyes by Bacterial Consortium.** *The Scientific World Journal* 2012; **2012**(1): 512454.

[33] Sartape AS, Mandhare AM, Jadhav VV, Raut PD, Anuse MA, Kolekar SS. **Removal of Malachite Green Dye from Aqueous Solution with Adsorption Technique Using Limonia acidissima (Wood Apple) Shell as Low Cost Adsorbent.** *Arabian Journal of Chemistry* 2017; **10**: S3229-S3238.

[34] Kumar R, Ahmad R. **Biosorption of Hazardous Crystal Violet Dye from Aqueous Solution onto Treated Ginger Waste (TGW).** *Desalination* 2011; **265**(1-3):112-118.

[35] Shamsipur M, Barati A, Nematifar Z. **Fluorescent pH Nanosensors: Design Strategies and Applications.** *Journal of Photochemistry and Photobiology C: Photochemistry Reviews* 2019; **39**:76-141.

[36] Bella F, Gerbaldi C, Barolo C, Grätzel M. **Aqueous Dye-Sensitized Solar Cells.** *Chemical Society Reviews* 2015; **44**(11):3431-3473.

[37] Silva F, Nascimento L, Brito M, da Silva K, Paschoal Jr W, Fujiyama R. **Biosorption of Methylene Blue Dye Using Natural Biosorbents Made from Weeds.** *Materials* 2019; **12**(15):2486, (1-16).

[38] Omer AM, Elgarhy GS, El-Subruiti GM, Khalifa RE, Eltaweil AS. **Fabrication of Novel Iminodiacetic Acid-Functionalized Carboxymethyl Cellulose Microbeads for Efficient Removal of Cationic Crystal Violet Dye from Aqueous Solutions.** *International Journal of Biological Macromolecules* 2020; **148**:1072-1083.

[39] Zhao D, Zhang W, Chen C, Wang X. **Adsorption of Methyl Orange Dye onto Multiwalled Carbon Nanotubes.** *Procedia Environmental Sciences* 2013; **18**:890-895.

[40] Muthukumaran C, Sivakumar VM, Thirumarimurugan M. **Adsorption Isotherms and Kinetic Studies of Crystal Violet Dye Removal from Aqueous Solution Using Surfactant**

Modified Magnetic Nanoadsorbent. *Journal of the Taiwan Institute of Chemical Engineers* 2016; **63**:354-362.

[41] Rangabhashiyam S, Lata S, Balasubramanian P. **Biosorption Characteristics of Methylene Blue and Malachite Green from Simulated Wastewater onto Carica papaya Wood Biosorbent.** *Surfaces and Interfaces* 2018; **10**:197-215.

[42] Zhou G, Wang KP, Liu HW, Wang L, Xiao XF, Dou DD, Fan YB. **Three-Dimensional Polylactic Acid@ Graphene Oxide/Chitosan Sponge Bionic Filter: Highly Efficient Adsorption of Crystal Violet Dye.** *International Journal of Biological Macromolecules* 2018; **113**:792-803.

[43] Boudrahem F, Aissani-Benissad F, Soualah A. **Removal of Basic Yellow Dye from Aqueous Solutions by Sorption onto Reed as an Adsorbent.** *Desalination and Water Treatment* 2015; **54**(6):1727-1734.

[44] Ayawei N, Ebelegi AN, Wankasi D. **Modelling and Interpretation of Adsorption Isotherms.** *Journal of Chemistry* 2017; **2017**(1): 3039817.

[45] Nyankson E, Adjasoo J, Efavi JK, Yaya A, Manu G, Kingsford A, Abrokwah RY. **Synthesis and Kinetic Adsorption Characteristics of Zeolite/CeO2 Nanocomposite.** *Scientific African* 2020; 7:e00257.

[46] Liu B, Luo H, Rong H, Zeng X, Wu K, Chen Z, Lu H, Xu D. **Temperature-Induced Adsorption and Desorption of Phosphate on Poly (Acrylic Acid-Co-N-[3-(Dimethylamino) Propyl] Acrylamide) Hydrogels in Aqueous Solutions.** *Desalination and Water Treatment* 2019; **160**:260-267.

[47] Ahmed M, Mashkoor F, Nasar A. **Development, Characterization, and Utilization of Magnetized Orange Peel Waste as a Novel Adsorbent for the Confiscation of Crystal Violet Dye from Aqueous Solution.** *Groundwater for Sustainable Development* 2020; **10**:100322.

[48] Laskar N, Kumar U. **Adsorption of Crystal Violet from Wastewater by Modified Bambusa tulda.** *KSCE Journal of Civil Engineering* 2018; **22**:2755-2763.

[49] Miyah Y, Lahrichi A, Idrissi M, Boujraf S, Taouda H, Zerrouq F. **Assessment of Adsorption Kinetics for Removal Potential of Crystal Violet Dye from Aqueous Solutions Using Moroccan Pyrophyllite.** *Journal of the Association of Arab Universities for Basic and Applied Sciences* 2017; **23**:20-28.

[50] Ahmed SH, Rasheed EA, Rasheed LA, Abdulrahim FR. **Decolorization of Cationic Dye from Aqueous Solution by Multiwalled Carbon Nanotubes.** *Journal of Ecological Engineering* 2024; **25**(2):72-84.